

Supplementary Information

Biocompatible *N*-carbazoleacetic acid decorated Cu_xO nanoparticles as self-cascading platforms for synergistic single near-infrared triggered phototherapy treating microbial infections

Xiao-Chan Yang,^a Yong Ding,^a Sheng-Nan Song,^a Wen-Hui Wang,^a Shan Huang,^{a,b} Xue-Yao Pang,^a Bo Li,^a Ya-Ya Yu,^a Ya-Mu Xia^{*a} and Wei-Wei Gao^{*a}

^a State Key Laboratory Base of Eco-chemical Engineering, College of Chemical Engineering, Qingdao University of Science and Technology, Qingdao 266042, China

^b The Third Affiliated Hospital of Xuzhou Medical University, Xuzhou 221000, China

* Corresponding Address:

gww501@qust.edu.cn (W.-W. Gao); xiayamu@126.com (Y.-M. Xia)

1. Chemicals and reagents

Hydrogen peroxide (30%), bromoacetic acid (98.5%), carbazole (98%), acetic acid (CH₃COOH), methanol (CH₃OH), ethanol (C₂H₅OH), hydrochloric acid (HCl), 5,5'-dithiobis(2-nitrobenzoic acid (DTNB), and *N,N*-dimethylformamide (DMF) were purchased from Sinopharm Chemical Reagent Co. Acetate monohydrate [Cu(OAc)₂•H₂O], 3-propyl-2-[5-(3-propyl-2(3H)-benzothiazolydene)-1,3-pentadien-1-yl]-iodide(1:1) [diSC3(5)], crystal violet (CV) and amplex red (AR) were obtained from Aladdin Reagent Co. 3,3',5,5'-Tetramethylbenzidine (TMB), *o*-phenylenediamine (OPD), tetramethylpiperidine (TEMP), 5,5-dimethyl-1-pyrroline-*N*-oxide (DMPO) and 1,3-diphenylisobenzofuran (DPBF) were achieved from Sigma-Aldrich. 4,6-Diamidino-2-phenylindole (DAPI) was purchased from Wuhan Chemstan Biotechnology Co., Ltd. Interleukin-10 (IL-10) and Tumor necrosis factor- α (TNF- α) were obtained from Beijing Bioss Biotechnology Co., Ltd. FITC conjugated goat anti-rabbit IgG was purchased from Servicebio. All other chemicals were reagent grade or better. All other reagents and solvents were used as received. The deionized water of resistivity 18.2 M Ω /cm was used in all experiments. *MRSA* and *AREC* were provided by Sichuan Provincial People's Hospital, Chengdu, China.

2. Apparatus

Scanning electron microscopy (SEM) images were obtained on a HITACHI Regulus 8100 at a working voltage of 15 kV after platinum coating for 45 s. Transmission electron microscopy (TEM), energy dispersive X-ray spectroscopy (EDS) and EDS element mapping were acquired on the JEOL JEM-F200. XPS (X-ray photoelectron spectrometry, AXIS

SUPRA) and XRD (X-ray diffraction, ULTIMALV) were employed to evaluate the phase composition of the samples on an X-ray diffractometer (Cu K α radiation, $k = 0.15406$ nm). Fourier transform-infrared (FT-IR) spectra were conducted on a Thermo Fisher Nicolet iS50 (KBr pellet technique ranging from 4000 to 400 cm^{-1} with a 2.0 cm^{-1} resolution). The concentration of the released Cu^{2+} ions was detected using inductively coupled plasma-atomic emission spectrometry (ICP-AES, AtomsScan Advantage). UV-Vis absorbance measurements were carried out on a PEERSEE TU-1810 UV-Vis spectrophotometer with a Peltier temperature control accessory and CARY5000 UV-Vis spectrophotometer with an integrating sphere. The fluorescence was tested by F-4700. The ζ -potential and size of the nanoparticles were measured in a Zetasizer 3000HS analyzer. All electron spin resonance (ESR) measurements were carried out on a JEOL JES FA200 spectrometer at ambient temperature.

3. GSH consumption

The GSH consumption assays of $\text{Cu}_x\text{O-CAA-1}$, $\text{Cu}_x\text{O-CAA-2}$, $\text{Cu}_x\text{O-CAA-3}$ and Cu_2O were detected by Ellman's assay. Ellman reagent DTNB reacted with thiol groups (-SH) in GSH to obtain a yellow product (TNB). $\text{Cu}_x\text{O-CAA-1}$, $\text{Cu}_x\text{O-CAA-2}$, $\text{Cu}_x\text{O-CAA-3}$ and Cu_2O were treated with GSH (100 μL , 10 mM) in PBS (1.85 mL, pH 8.0) under 20 $^\circ\text{C}$ and 40 $^\circ\text{C}$ water bath environment. DTNB (10 μL , 10 mM) was added at different time respectively for mixing. Next, the mixture solution was centrifuged and the supernatant was required to measure GSH consumption through UV-vis absorption (at 412 nm for TNB) to study the concentration-dependent and time-dependent consumption of GSH. The loss of GSH was calculated as follows:

$$\text{Loss of GSH (\%)} = (A_n - A_s) / A_n \times 100 \quad (\text{S1})$$

where A_s is the absorbance of the sample and A_n is the absorbance of the negative control. All assays were performed as triplicates.

4. GSH-OXD-like catalytic activity of $\text{Cu}_x\text{O-CAA-3}$ and kinetic assay

Amplex red (AR) was used as a fluorescence probe. In brief, $\text{Cu}_x\text{O-CAA-3}$ (0, 40, 80, 160 $\mu\text{g/mL}$) with GSH (1 mM) were mixed with AR (0.2 mg/mL) in 0.2 M PBS (pH 4.0) for 50 min. The fluorescence spectrum of the mixed solution was measured by using a fluorescence spectrophotometer, where the maximum excitation wavelength was 571 nm and the maximum emission wavelength was 585nm. To test whether O_2 is required for the reaction, the mixture reacted in air, O_2 , and N_2 atmosphere, respectively.

For kinetic assay, the Michaelis constant (K_M) is defined as the substrate concentration at half the maximum reaction rate. K_M reflects the affinity of $\text{Cu}_x\text{O-CAA-3}$ for its substrate. Maximal reaction velocity (V_{max}) is the maximal reaction

rate that is observed at saturating substrate concentrations. The kinetics constants K_M and V_{max} were calculated through fitting the initial reaction velocity values (V) and the substrate concentrations to equations S2-S4.

$$V = (V_{max} \times [S]) / (K_M + [S]) \quad (S2)$$

where $[S]$ is the concentration of substrate, V is the initial velocity and is calculated using the following equation:

$$V = \Delta A / (\Delta t \times \epsilon \times l) \quad (S3)$$

where ΔA is the change of absorbance value, Δt is the initial reaction time (s), ϵ is the molar absorption coefficient of the colorimetric substrate, and l is the path length of light traveling in the cuvette (cm).

The catalytic constant (k_{cat}) is defined as the maximum number of substrate molecules converted to product per unit of time and is calculated by the following equation:

$$k_{cat} = V_{max} / [E] \quad (S4)$$

where $[E]$ is the concentration of Cu_xO-CAA-3 (M).

k_{cat}/K_M characterizes both the affinity and catalytic ability of the enzyme to the substrate, reflecting the catalytic efficiency of Cu_xO-CAA-3. The kinetic assay was performed in the reaction of Cu_xO-CAA-3 (40 µg/mL) with different concentrations of GSH (0.1, 0.2, 0.4, 0.6, 0.8 mM).

5. POD-like catalytic activity of Cu_xO-CAA NPs and kinetic assay

The POD-like activity assays of Cu_xO-CAA-1, Cu_xO-CAA-2, Cu_xO-CAA-3 and Cu₂O were carried out using TMB and OPD as the reagents in the presence of H₂O₂ in 0.12 M acetate buffer solution (pH 4.0). The UV-vis absorbance of the color reaction (at 652 nm for TMB and at 425 nm for OPD) was recorded at a certain reaction time to express the POD-like activity. The steady-state kinetic assay of Cu_xO-CAA-3 with H₂O₂ as the substrate was performed by adding 50 µg/mL Cu_xO-CAA-3 into 0.2 M HAc-NaAc buffer solution (pH 4.0) containing TMB (1 mM) and different concentrations of H₂O₂ (0.25, 0.5, 1, 2, 4, 8 mM).

6. Photothermal performance of Cu_xO-CAA NPs

Cu_xO-CAA-1, Cu_xO-CAA-2, Cu_xO-CAA-3 and Cu₂O (31.25, 62.5, 125, 250 and 500 µg/mL) were irradiated by 808 nm NIR (1.0 W/cm²) for 600 s, with a temperature measured at 30 s intervals, after which the NIR irradiation is switched off and the temperature is measured at 30 s intervals until 600 s. Temperature measurement using thermocouple probes. Cu_xO-CAA-3 aqueous dispersion (0.2 mL) at a concentration of 62.5 µg/mL was exposed to 808 nm laser irradiation for 600 s, then the laser was switched off and cooled to room temperature to determine its photothermal stability.

7. Calculation of the photothermal conversion efficiency (η) of Cu₂O and Cu_xO-CAA-3

The heating and cooling temperature variation patterns for 62.5 µg/mL Cu₂O and Cu_xO-CAA-3 above were used to calculate the η for Cu₂O and Cu_xO-CAA-3 according to the following equations:

$$\eta = [h(T_{max} - T_{surr}) - Q_{diss}] / I(1 - 10^{-A_{808}}) \quad (S5)$$

$$\tau_s = mC_p / hS \quad (S6)$$

where h is the heat-transfer coefficient, S is the surface area of the container, T_{max} is the equilibrium temperature, T_{surr} is the ambient temperature, Q_{diss} is the heat obtained by container under 808 nm laser irradiation, I is the density of laser power, A_{808} is the absorbance of the Cu₂O and Cu_xO-CAA-3 suspension at 808 nm, and τ_s is the time constant obtained from Figure 4f and S6c, respectively.

8. Photodynamic effect of Cu_xO-CAA NPs

The photodynamic activity of Cu_xO-CAA-1, Cu_xO-CAA-2, Cu_xO-CAA-3 and Cu₂O were assessed by the degradation of DPBF under 808 nm NIR (1.0 W/cm²). Cu_xO-CAA-1, Cu_xO-CAA-2, Cu_xO-CAA-3 and Cu₂O were added to their respective DMF (30 mL) with DPBF (7 mg) and stirred in the dark for 10 min. After NIR irradiation, the photoreactive solution (2 mL) was separated by centrifuging for 4000×g for 5 min to remove the particles. Then the absorbance at 425 nm was measured separately at a UV-Vis spectrophotometer.

9. ROS detection by ESR

5,5-Dimethyl-1-pyrroline-*N*-oxide (DMPO) was used to detect •OH, 2,2,6,6-tetramethylpiperidine (TEMP) was used to detect ¹O₂. 10 µL of DMPO was mixed with 50 µL of Cu_xO-CAA-3 (50 µg/mL). 10 µL of TEMP was mixed with 100 µL of Cu_xO-CAA-3 (50 µg/mL). The mixture was placed into a quartz capillary for detection. For the H₂O₂ containing group, 8 mM of H₂O₂ was added in mixture. For the NIR group, 808 nm laser (1.0 W/cm², 5 min) was used to irradiate the mixture before detection.

10. Cu²⁺ release

Cu₂O (5 mL, 0.5 mg/mL) and Cu_xO-CAA-3 (5 mL, 0.5 mg/mL) solutions were respectively mixed with aqueous hydrochloric acid (pH 4.0) and PBS (pH 7.0). The mixture was placed on a shaker and taken out at the specified time point, then centrifuged at 7000 rpm for 5 min to obtain the supernatant for ICP-AES test.

11. Protein leakage

MRSA and *AREC* cells (10⁶ CFU/mL) were treated with increasing concentrations of Cu_xO-CAA-3 for 1 h at 37 °C and then irradiated for 5 min under 808 nm NIR (1.0 W/cm²). Subsequently, the cells were pelleted down at 4000 rpm

for 8 min, and the cell-free supernatant was collected. The concentration of leaked proteins in the supernatant was measured using the standard Bradford assay.

12. Cytoplasmic membrane depolarization

The membrane potential-sensitive fluorescent dye, DiSC3(5), was employed as an indicator of membrane depolarization. *MRSA* and *AREC* in the exponential growth phase was diluted to 10^8 CFU/mL and washed twice with saline. The potentiometric probe DiSC3(5) was added to the bacterial suspension at a final concentration of 1 μ M until a stable value of fluorescence was achieved (E_x : 620 nm, E_m : 680 nm). Cu_xO -CAA-3 at final concentrations of 5 μ g/mL (0.5 MIC), 10 μ g/mL (1 MIC), 20 μ g/mL (2 MIC), 40 μ g/mL (4 MIC) and 80 μ g/mL (8 MIC) was added to the medium containing the bacteria and DiSC3(5), and the fluorescence intensity was monitored using a microplate reader. Triton X-100 (0.1 %) was employed as the positive control.

13. Antibiofilm

Overnight cultured bacteria were diluted in a fresh LB broth and cultured to the mid log phase, then resuspended in fresh medium (OD_{600} of approximately 0.1). Aliquots of 100 μ L of bacterial suspension and final concentrations of 0, 5, 10, 20, 40 and 80 μ g/mL of Cu_xO -CAA-3 were co-stored in a 96-well plate at 37 °C for 24 h, and irradiated every 12 h for 10 min under 808 nm NIR (1.0 W/cm²). The medium was removed from the wells and the biofilm was carefully washed twice with PBS to remove planktonic bacteria. The biofilms were fixed with 10% ethanol for 10 min, and then stained with 0.1% CV for 30 min in each well. After discarding CV, the biofilm samples were washed with PBS, and 33% AcOH was added to dissolve the fuel on the biofilm, then the absorbance at 570 nm was measured using a microplate reader. The calculation formula of relative biofilm biomass is calculated as follows:

$$Relative\ biofilm\ biomass\ (\%) = (A_1 - A_2) / A_1 \times 100 \quad (S7)$$

where A_1 represents positive control and A_2 represents experiment group.

14. Bacterial resistance

The strains of *MRSA* and *AREC* were exposed to Cu_xO -CAA-3+NIR group for sustained passages, and then the MIC of Cu_xO -CAA-3 was determined against each passage of the strain. The freshly diluted *MRSA* (10^5 CFU/mL) and *AREC* (10^5 CFU/mL) in the broth medium were respectively cultured in 10 μ g/mL Cu_xO -CAA-3+NIR (808 nm, 1.0 W/cm², 5 min) at 37 °C for 12 h on a shaker bed at 90 rpm, and the sensitivity of each strain passage to Cu_xO -CAA-3 was tested. For comparative analysis, ceftizoxime was used as a control.

15. Antibacterial experiments *in vitro*

The antibacterial ability of Cu_xO-CAA-3 was determined by plate counting method. Briefly, bacteria suspensions (10⁸ CFU/mL, 100 μL) were incubated with CAA (50 μg/mL), Cu₂O (10 μg/mL), and Cu_xO-CAA-3 (10 μg/mL) in a 96-well plate respectively. PBS was used as the control. An 808nm laser light (1.0 W/cm²) irradiated the NIR group for 5 min. After incubated at 37 °C for 45 min, the bacteria suspension (diluted by 1-10⁴ fold, 100 μL) was spread on the LB agar plates. The number of bacteria colonies was counted and recorded after incubation for 24 h at 37 °C.

16. Cytotoxicity measurement

Cytotoxicity evaluation was performed on Human umbilical vein endothelial cells lines (HUVEC). These cells were implanted into 96-well microplates and permitted to adhere overnight. Subsequently, the culture medium was substituted by fresh culture medium including Cu_xO-CAA-3 (0-8 MIC)+NIR (808 nm, 1.0 W/cm², 5 min). After the co-incubation for 24 h, the culture medium was substituted by MTT (20 μg/mL) culture solution and incubation for 4 h. Ultimately, DMSO (150 μL) was added to each well. Cell viability was calculated by measuring the absorbance at λ = 490 nm to the control via a microplate reader.

17. Hemolysis

Fresh blood from mice was taken and erythrocytes were isolated by centrifugation (4000 rpm, 3 min). The obtained erythrocytes were washed three times with saline and then diluted to a final concentration of 5% (v/v). Cu_xO-CAA-3 (500 μL) with erythrocyte solution (500 μL) was added into a 24-well microtiter plate and then shaken at 100 rpm for 2 h in an incubator at 37 °C. Afterwards, the microplate contents were centrifuged (4000 rpm, 3 min) and the supernatant (100 μL) was introduced into a 96-well microplate. The absorbance of the solution at 540 nm was determined using a microplate reader. Triton X-100 (0.1%) was used as a positive control. The hemolysis rate is calculated as follows:

$$\text{Hemolysis rate (\%)} = (A_p - A_b) / (A_t - A_b) \times 100 \quad (\text{S8})$$

where A_p represents the experimental group, A_t represents the positive control and A_b represents blank control.

18. Mice wound model

All animal experiments in this study were approved and compliant with the guidelines of the Institutional Animal Care and Use Committee (IACUC) of Qingdao University of Science and Technology. The wound model was built on the back of male Kunming mice (18-22 g, 4-5 weeks old), which were purchased from the Model Animal Research Center (MARC) of Ji Nan PengYue Co. Ltd. (Ji Nan, China). The mice were slashed with 9 mm diameter round wound and *MRSA* cells

(1×10^8 CFU/mL, 20 μ L) were injected into the wound for constructing the infected wound model. After 24 h, the infected mice were respectively treated with PBS, CAA, Cu₂O and Cu_xO-CAA-3. Meanwhile, photographs of the wounds were taken every day. For histological analysis, the mice were sacrificed with an overdose of pentobarbital (100 mg/kg) on day 14. The entire wound with adjacent normal skin was collected and fixed using 4% paraformaldehyde solution for 24 h at 4 °C. The sample of subcutaneous tissue was analyzed using H&E staining method. All sections were observed and photographed with a microscope (BX51, Olympus, Japan), meanwhile, the wound was excised and incubated in sterile saline for 24 h at 37 °C. Then, the culture solution was diluted 10³-fold and cultured on LB agar plates at 37 °C for 24 h for counting the number of bacterial colonies. The wound healing rate was calculated as follows:

$$\text{Wound healing rate (\%)} = (A_{\text{initial}} - A_{\text{time}}) / A_{\text{initial}} \times 100 \quad (\text{S9})$$

where A_{initial} is the initial wound area (day 0), and A_{time} is the wound area at different time points.

19. Immunofluorescence analysis

Paraffin tissues slices were deparaffinized, and washed three times by PBS for 5 min each time, then blocked and permeabilized with bovine serum albumin (5%) and 0.5 % Triton X-100 for 30 min. Next, tissues slices were incubated with primary antibodies overnight at 4 °C. After washing three times by PBS, the slices were incubated in the blocking buffer containing corresponding fluorophore-conjugated secondary antibodies for 50 min at room temperature. Tissues slices were washed three times with PBS again, then stained with DAPI and incubated with antifade solution to reduce autofluorescence using for immunofluorescence images.

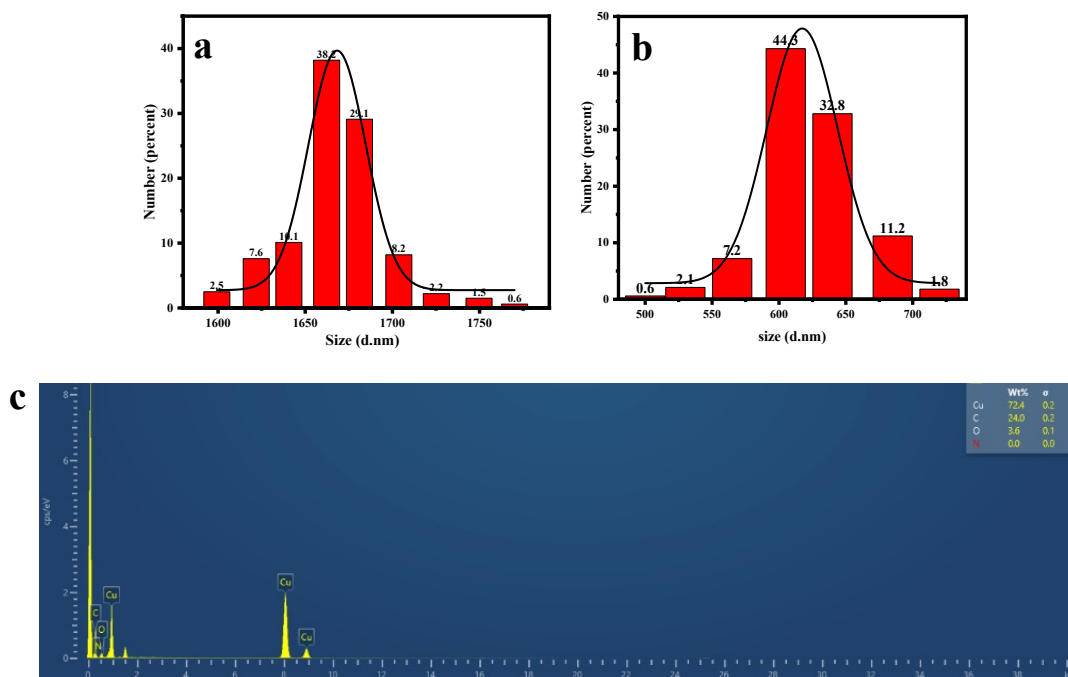


Figure S1 The size distribution histogram of (a) Cu₂O and (b) Cu_xO-CAA-3; (c) EDS mapping of Cu_xO-CAA-3.

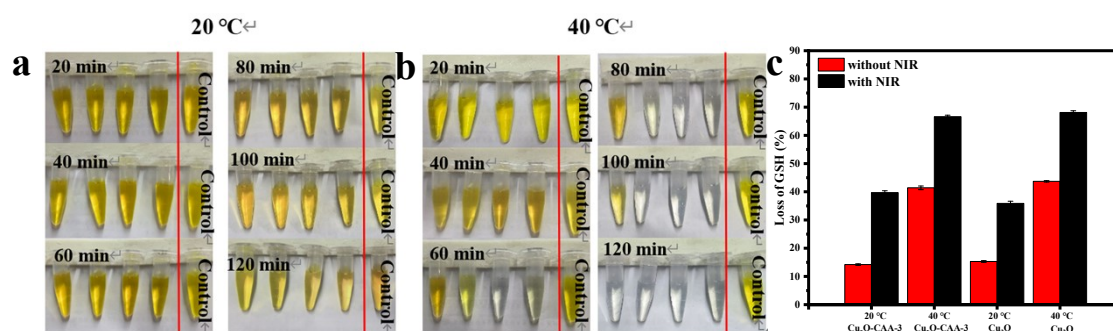


Figure S2 Photographs for the color change after GSH oxidation with Cu_xO-CAA-3 (40 μg/mL) at different time intervals determined by Ellman's assay at (a) 20 °C and (b) 40 °C; (c) Loss of GSH plots measured at 20 °C and 40 °C in a water bath after 30 min of irradiation (808 nm, 1.0 W/cm²) for Cu_xO-CAA-3 (40 μg/mL) and Cu₂O (40 μg/mL).

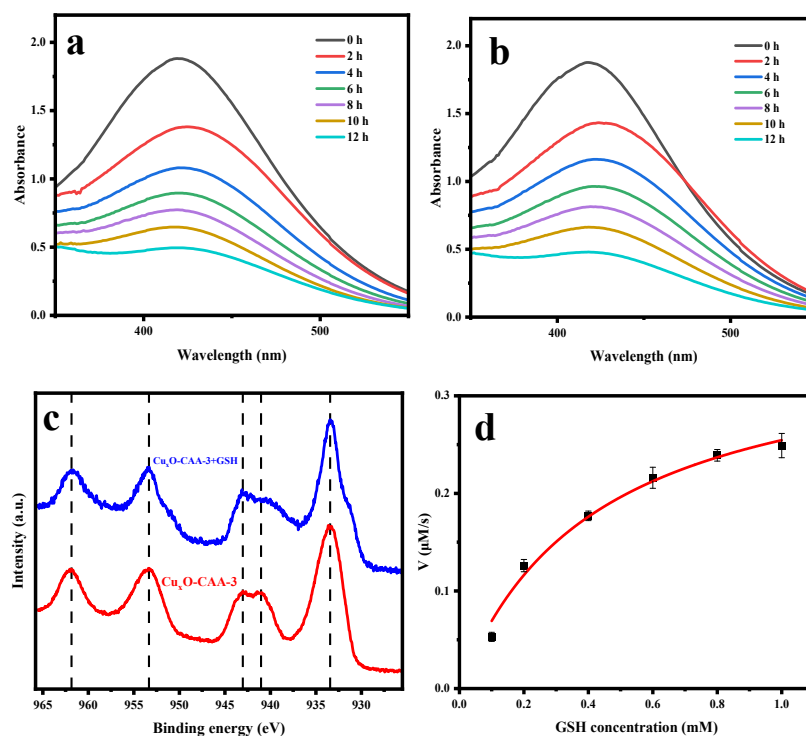


Figure S3 Time-dependent GSH depletion by (a) Cu_xO-CAA-3 (10 μg/mL) and (b) Cu₂O (10 μg/mL); (c) Cu 2p core-level XPS spectra of Cu_xO-CAA-3 (40 μg/mL) after incubation with GSH (1 mM) for 45 min; (d) Kinetic assay for the GSH-OXD-like activity of Cu_xO-CAA-3 with GSH as substrate.

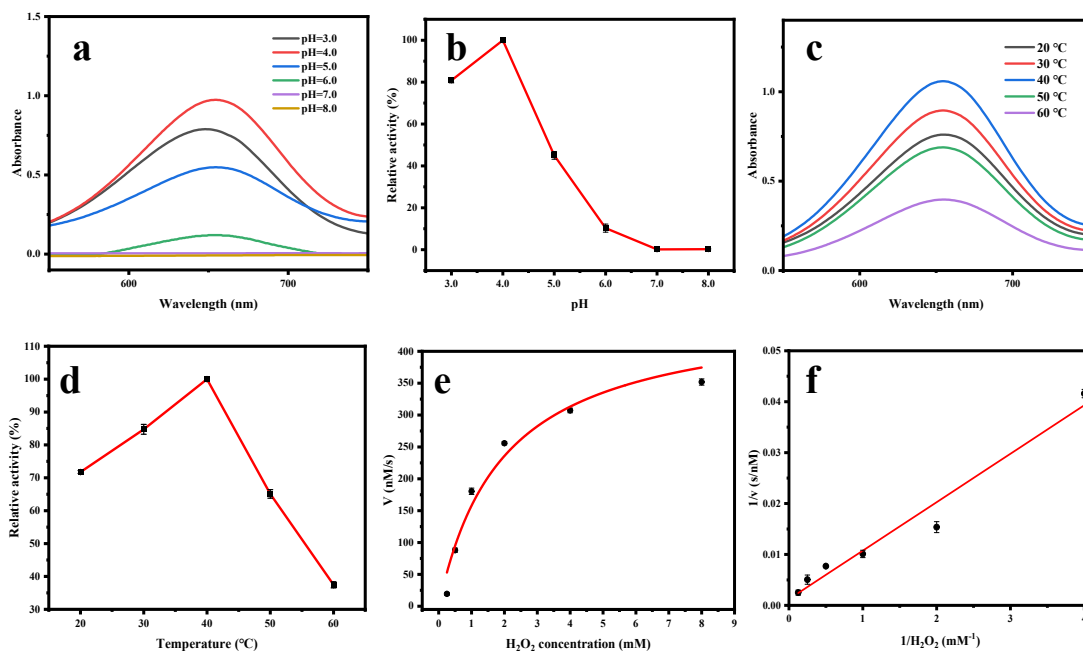


Figure S4 UV-vis absorption spectra of TMB+Cu_xO-CAA-3+H₂O₂ system at different (a) pH values and (c) temperatures; Effect of pH (b) and temperature (d) on the POD-like catalytic performance of Cu_xO-CAA-3; (e) Kinetic assay for the POD-like activity of Cu_xO-CAA-3 with H₂O₂ as substrate; (f) Corresponding double-reciprocal plots of POD-like activity of Cu_xO-CAA-3 at a fixed concentration of TMB (1 mM) versus varying concentration of H₂O₂ (0.25, 0.5, 1, 2, 4, 8 mM), data presented as mean ± SD (n=3).

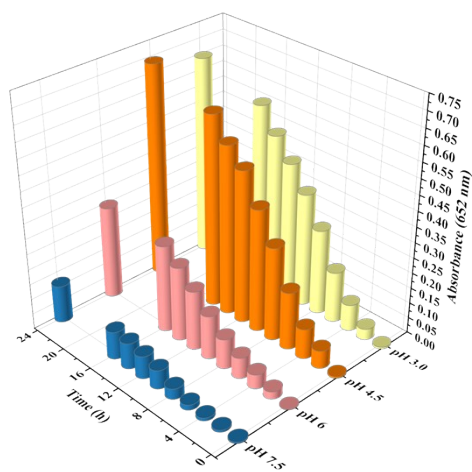


Figure S5 UV-vis absorption at 652 nm of TMB (1 mM)+Cu_xO-CAA-3 (200 µg/mL)+GSH (10 mM) system with different pH values (3.0, 4.5, 6.0, 7.5) for 2 h, 4 h, 8 h, 10 h, 12 h, 14 h, 16 h and 24 h, respectively, the operating temperature is 40 °C.

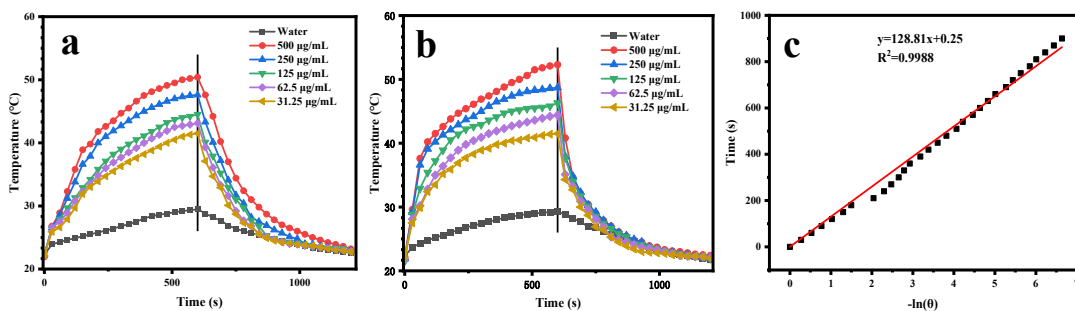


Figure S6 Temperature change curves of (a) Cu_xO -CAA-1 and (b) Cu_xO -CAA-2 aqueous solutions with different concentrations (808 nm laser irradiation for 600 s and then turned off the NIR laser for 600 s); (c) The cooling time plot after 600 s vs the negative natural logarithm of driving force temperature ($-\ln\theta$) with slope of 128.81 for 62.5 $\mu\text{g/mL}$ of Cu_2O .

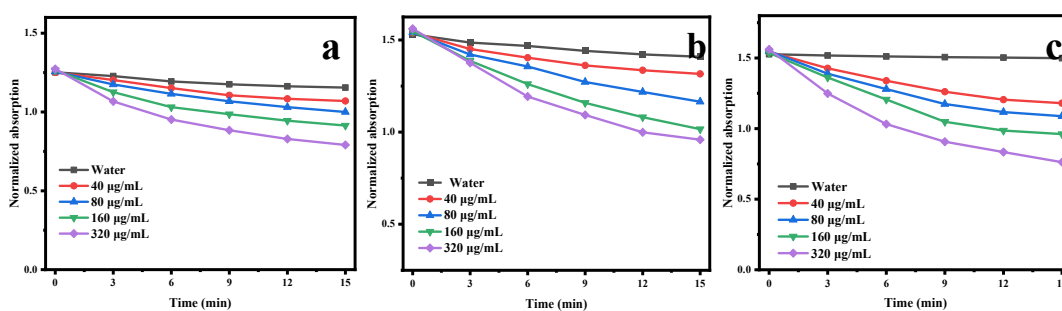


Figure S7 UV-vis absorption intensity of DPBF at 415 nm in the presence of different concentrations of (a) Cu_2O , (b) Cu_xO -CAA-1 and (c) Cu_xO -CAA-2 with NIR irradiation (808 nm, 1.0 W/cm^2).

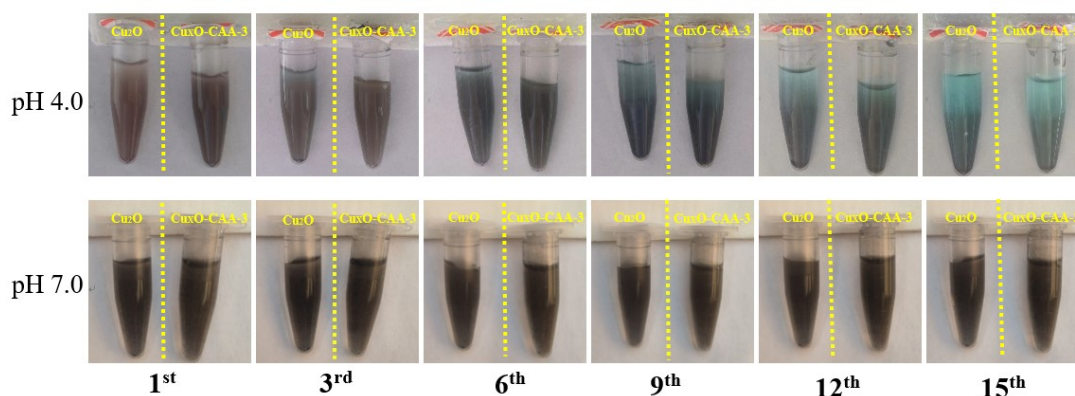


Figure S8 Photographs for the color change of Cu_2O and Cu_xO -CAA-3 solutions (pH 4.0 and 7.0) after 1, 3, 6, 9, 12, and 15 days' storage.

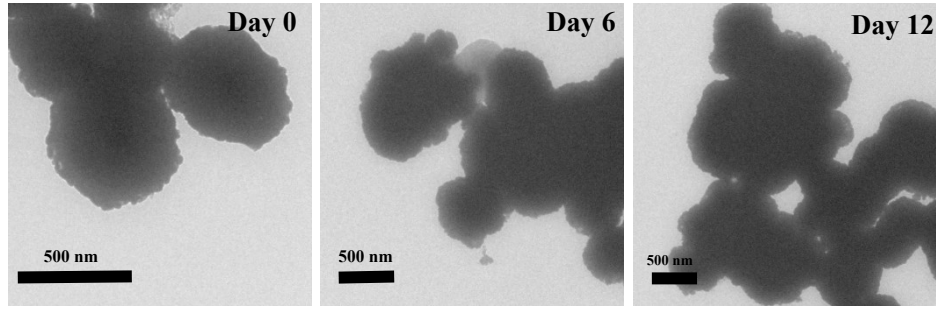


Figure S9 TEM images of Cu_xO -CAA-3 stored in pH 4.0 solution for 0, 6, 12 days.

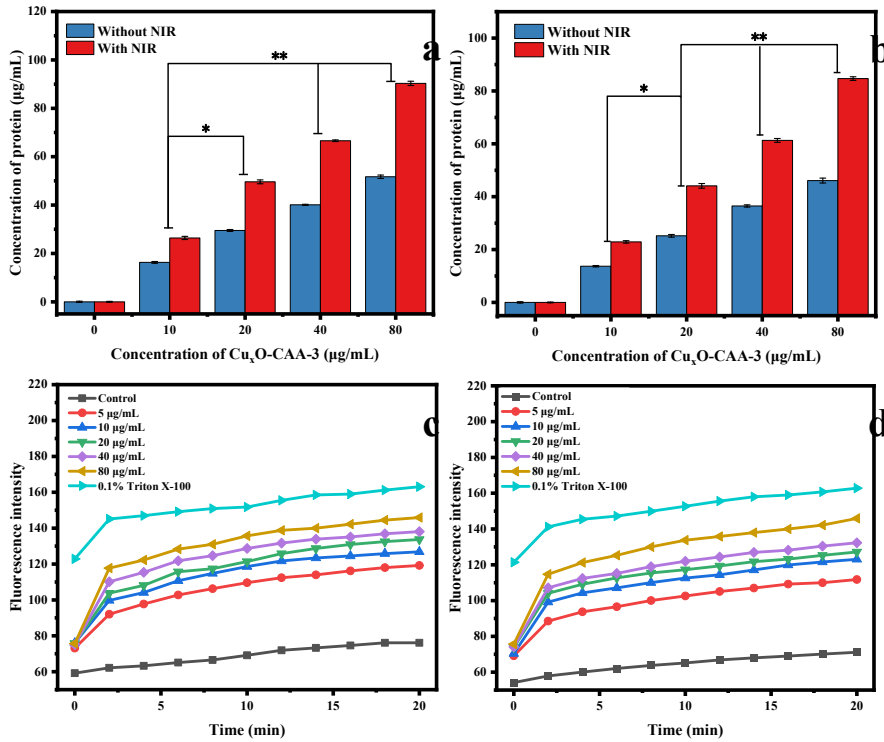


Figure S10 Protein leakages of (a) *MRSA* and (b) *AREC* treated with Cu_xO -CAA-3+NIR; Membrane depolarization of (c) *MRSA* and (d) *AREC* in the presence of Cu_xO -CAA-3 with NIR. All groups requiring NIR irradiation were irradiated under an 808 nm laser (1.0 W/cm^2) for 5 min.

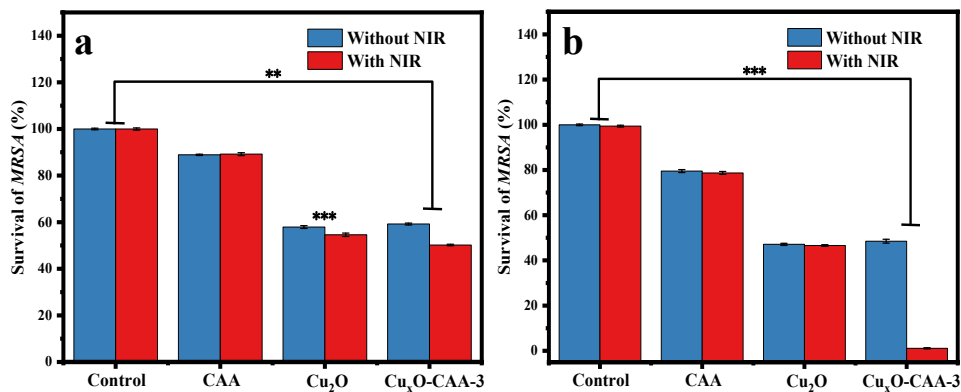


Figure S11 Quantitative analysis of *MRSA* colonies on days (a) 3 and (b) 9. Data presented as mean \pm SD (n=3), asterisks indicate significant differences (* p < 0.05, ** p < 0.01, *** p < 0.001).

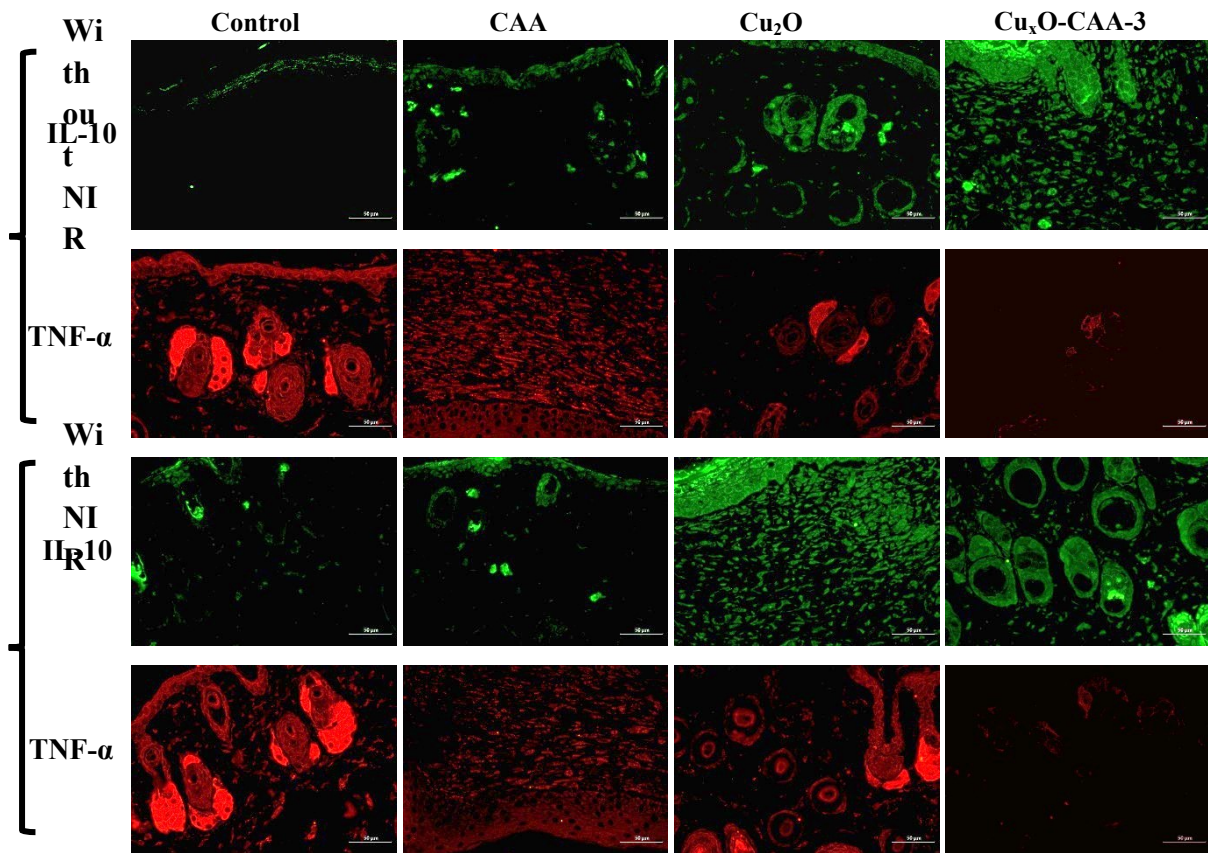
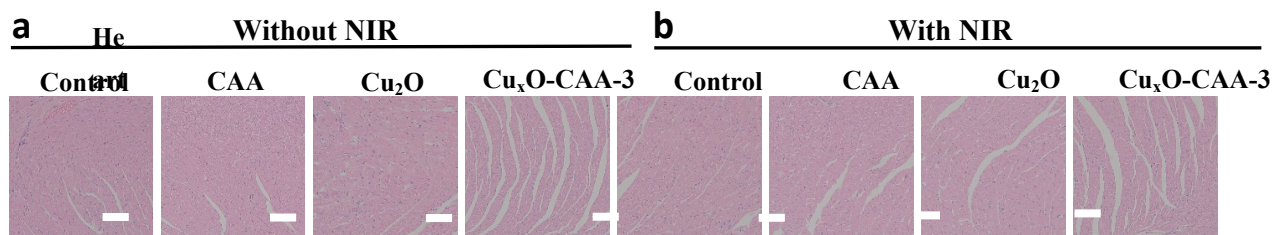


Figure S12 Immunofluorescence staining of IL-10 (green) and TNF- α (red) in granulation tissues on day 9 (scale bars represent 50 μ m). NIR: 808 nm, 1.0 W/cm², 5 min.



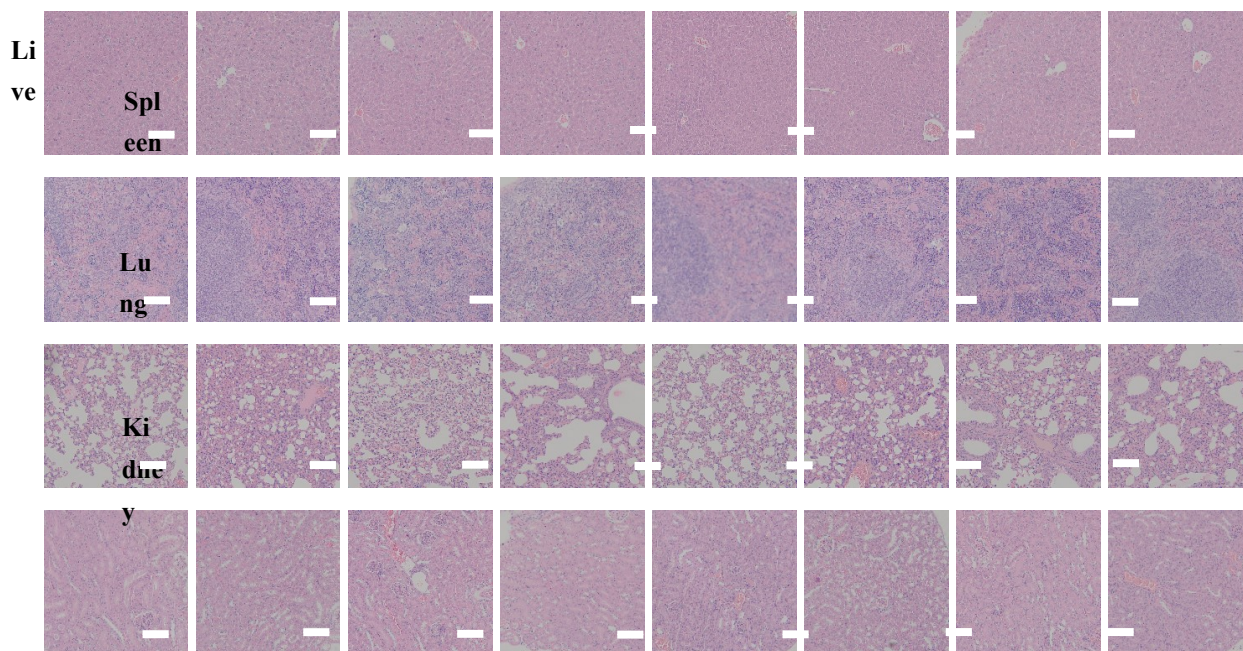


Figure S13 Histological studies with H&E staining. Heart, liver, spleen, lung and kidney are dissected from mice after 9 days' treatment (scale bars represent 100 μm).

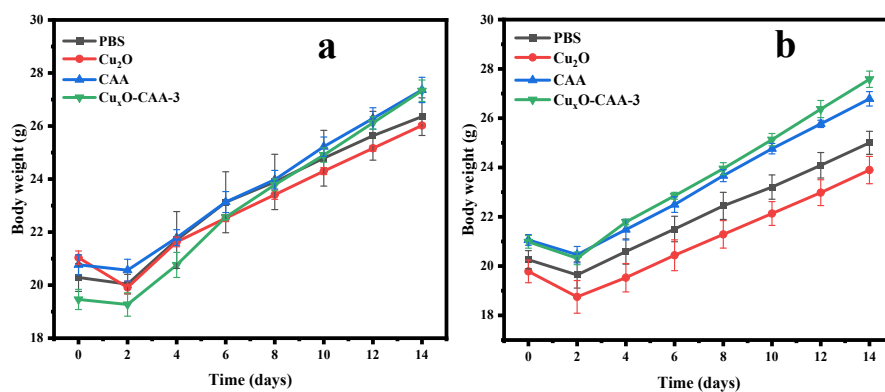


Figure S14 Body weight changes of mice after various treatments (a) with and (b) without NIR (808 nm, 1.0 W/cm², 5 min). Data presented as mean \pm SD (n=3).